Journal of Power Sources 180 (2008) 452–460

Contents lists available at ScienceDirect

Journal of Power Sources

journal homepage: www.elsevier.com/locate/jpowsour

PEM fuel cell stack testing in the framework of an EU-harmonized fuel cell testing protocol: Results for an 11 kW stack

Roberto Bove*, Thomas Malkow, Antonio Saturnio, Georgios Tsotridis

European Commission, Directorate-General Joint Research Centre, Institute for Energy, PO Box 2, 1755 ZG Petten, The Netherlands

ARTICLE INFO

Article history:
Received 17 September 2007
Received in revised form 18 January 2008
Accepted 10 February 2008
Available online 10 March 2008

Keywords:
Testing
PEFC stack
Test protocols
Harmonized test

ABSTRACT

Fuel cell testing and standardization thematic network (FCTESTNET) was a Thematic Network funded by the European Commission under the Fifth Framework Program (FP5), which was comprised of 55 European partners. The project concluded in 2006 and the main output was the collection and compilation of agreed testing procedures for different fuel cell technologies (PEM, SOFC, MCFC), applications (stationary, portable, transport), as well as balance of plant.

Experimental validation of such testing procedures is the next necessary step for obtaining reliable harmonized testing procedures. The Joint Research Centre (JRC), Institute for Energy (IE) has started the validation process on selected PEM testing procedures. One of the FCTESTNET procedures applied at JRC-IE is the polarization curve for a PEM stack. Results show that the harmonization of some parameters, such as the acquisition and equilibrium time for each value of the current density, and the control of the stack coolant temperature, is a necessary action for an objective and trustworthy comparison of the performance data.

1. Introduction

Although fuel cells can play a relevant role in an energy scenario characterized by improved sustainability, security of supply and economical competitiveness, the technology is not yet mature enough for end user applications on the wide scale, and needs to be further developed. For the rating of improvements in fuel cell technology, common agreed measures for system efficiency, power density, dynamic behavior and durability are indispensable. This requires the definition of harmonized, validated and benchmarked testing procedures for entire fuel cell systems as well as system components, so that the tremendous variety of boundary conditions – e.g. caused by different applications, stack technologies, types of fuel, fuel quality – can be traced back to a common agreed basis. The need of such harmonized testing procedures is evident even for the relatively simple and widely employed polarization test.

A polarization curve is defined as the "typical plot of cell voltage as a function of current density" [1]. This test is performed for a variety of reasons, primarily for rating the expected performance, in terms of voltage and power, of a single cell or stack under certain operating conditions. Very frequently, polarization curves are employed to compare the performance related to different cell materials or designs (e.g. [2–6]), to verify the quality of the manufacturing process (acceptance test), or to compare the performance of a specific fuel cell under different operating conditions, such as relative humidity of the gas streams, fuel cell temperature and pressure, and gas composition [7–11].

Especially if employed for performance comparison, it is imperative that all the boundary conditions applied to the testing system are precisely the same. Santarelli and Torchio [8], for example, attempt to compare the results of their experimental campaign with data available in the literature. However, they notice that polarization curves are usually obtained by applying operating parameters that are different among different authors. In addition, several authors do not report the procedure and the operating conditions applied for the tests, thus the mere comparison of the resulting polarization curves would be erroneous and misleading.

As the polarization curve is only one of the tests being performed on fuel cells, it is obvious that the harmonization of the testing procedures is a long and time-consuming process. Moreover, in order to be widely accepted, it requires international consensus. To create a common language among different institutions performing fuel cell tests, several international activities have been initiated, with the main aim of setting-up testing procedures that allow a transparent and objective interpretation of the results.

The present paper is organized as follows: Section 2 describes the main international activities dealing with the testing procedures harmonization and standardization; Section 3 presents the experimental activity conducted at JRC-IE on an 11 kW_e stack for the

* Corresponding author. Tel.: +31 22456 5101; fax: +31 22456 5623.
E-mail address: roberto.bove@jrc.nl (R. Bove).

0378-7753/$ – see front matter © 2008 Elsevier B.V. All rights reserved.
doi:10.1016/j.jpowsour.2008.02.032

validation of a polarization curve test module. Finally, in Section 4, the main findings of the experimental campaign are discussed.

2. International efforts in FC testing harmonization and standardization

At present, very few Regulations, Codes and Standards (RC&S) exist in the field of fuel cells. So far only a few major documents have been published: (e.g. [1,12–32]), but several working groups of standardization bodies have been set up and are dealing with this topic.

The preparation of International Standards for fuel cell technologies is the scope of the Technical Committee TC 105 "Fuel cell technologies" of the International Electrotechnical Commission (IEC). IEC operates in collaboration with the International Organization for Standardization (ISO), in particular on standardization activities related to automotive applications (ISO TC22 "Road Vehicles"/SC21 "Electrically propelled road vehicles") and hydrogen (ISO TC197 "Hydrogen technologies").

In parallel with international efforts, national regulations, codes and standards are being prepared in several countries, particularly in North America, Japan and Germany [16–31]. The content of the national RC&S spans from performance testing to safety requirements, including system installation guidelines and fuel metering. For the content of each single standard (or technical specification), the reader is referred to the specific documents [16–31].

As experimental tests are beyond the activities of most of the standards' working groups, several pre-normative projects are being undertaken to provide technical support to various national or international Standard Development Organizations (SDOs).

North America and Japan are particularly active in the pre-normative work for fuel cell testing. In the US, the US Fuel Cell Council has defined a number of testing procedures for fuel cell components and single cells [29,30], while for automotive applications, most of the activities are being undertaken by the Japanese Automotive Research Institute (JARI) [33,34]. JARI is particularly active in the definition of testing procedures for PEFC single cells and components, as well as the definition of hydrogen fuel quality for PEFC, intended for automotive applications [35,36].

Recently, JARI and the Hawaii Natural Energy Institute (HNEI) of the University of Hawaii at Manoa performed round-robin-testing on single cells, using JARI's testing protocol on polarization curve. Tests were performed at the JARI and HNEI facilities. This exercise showed a good reproducibility of the results, thus revealing the JARI test protocol as a solid base for the standardization process [37].

Within the Fifth Framework Programme (FP5), the European Commission financed the Thematic Network FCTESTNET, which involved 55 European Partners for harmonizing fuel cell testing procedures. As a follow-up of FCTESTNET within the Sixth Framework Programme (FP6), the project Fuel Cell Testing, Safety and Quality Assurance ($FCTES^{QA}$) provides experimental validation of the testing procedures defined in FCTESTNET. The experimental activities reported in the present paper have been conducted in the framework of FCTESTNET and $FCTES^{QA}$.

3. Experimental activity

3.1. Fuel cell testing facility and test object

At JRC, Institute for Energy, a fuel cell testing facility was established in 2005. The main purpose of the testing facility is to constitute an EC reference laboratory for fuel cell performance, available to the scientific community and industry. The facility supports the development of RC&S within the European Hydrogen and Fuel Cells Platform (HFP) and, at global level, in the frame of the International Partnership for the Hydrogen Economy (IPHE). Furthermore, it provides the opportunity for training and exchange of research fellows and scientists, thus strengthening the European Research Area (ERA) concept.

The facility allows testing and evaluation of PEM at conditions that typically exist in stationary and transport applications. In particular, the facility is capable of testing PEM stacks with nominal power up to 100 kW_e. The electricity generated during the tests can be dissipated through an external electrical load, or can be connected to the institute electrical grid, after power conditioning. In order to reproduce a wide range of applications, i.e. stationary and transport in different environmental conditions, the testing facility is equipped with an environmental chamber, where the temperature can be controlled in a range of −40 to +60 °C, with a relative humidity of up to 95%. A vibrating table, capable of producing shocks and vibrations with 6 degrees of freedom at a frequency of up to 250 Hz, is embedded in the environmental chamber. It should be noted that, in the present test campaign, the environmental chamber is employed for ensuring the specified ambient conditions, while no vibration is produced with the vibrating table.

The required flow of fuel and oxidant is regulated by respectively one and three mass flow controllers (MFCs) of Brooks Instrument (Brooks Smart Series-TMF). The MFCs are connected to field point I/O interface modules of National Instruments operated via RS-232 communications by a PC using an operation and control-based LabView software. The H_2 MFC has a range of 0–1600 nlpm (normal litres per minute) while the air-flow rate is regulated by three MFCs each of 0–2200 nlpm range. The PC software regulates the air flow by one MFC for up to 600 nlpm and by all three MFCs when this figure is exceeded. The flow rate accuracy is 1% of the full scale of the MFC. The uncertainty of the actual flow rate is thus depended on the MFC range employed. The humidification of the anodic and cathodic gases (H_2 and air) is carried out by mixing them with 180 °C hot steam and with a subsequent quenching of the mixtures in condensing heat exchangers. After removing the excess water via this heat exchanger, the humid gases are re-heated to the dew point temperatures set, using gas/oil heat exchangers.

The electricity generated during testing is fed to the building grid of the laboratory using a 120-kV A dc/ac electronic load inverter. The stack used for the tests contains 90 individual cells of 200 cm^2, separated by graphite bipolar plates, containing almost parallel flow patterns in Z-shaped geometry (Fig. 1). The stack is manufactured by NedStack Fuel Cell Technology BV of Arnhem, The Netherlands. It weighs about 35 kg and has dimensions of (length × width × height) 70 cm × 35 cm × 20 cm. The waste heat is removed from the fuel cell stack by DI water flowing inside the bipolar plates. This heat and that from the test equipment and ancillaries is dissipated using a water-cooling circuitry. The de-ionized water used to cool the stack to a certain temperature and to heat it up during start-up phase, is produced from tap water by reverse osmosis employing an ionomer membrane followed by a patented electro-deionization process. The so-produced deionized water has an ionic conductivity of 0.1 $\mu S\,cm^{-1}$ and is treated by ozone and ultraviolet radiation prior to its use to prevent microbial contamination.

3.2. Test module

The test module chosen for validation is the TM PEFC 5-3, i.e. polarization curve for a PEFC stack. Although polarization curves are widely used by several organizations as a tool for performance benchmarking, these are not always obtained applying the same

Fig. 1. PEFC stack used for the tests.

boundary conditions to the test object. A typical issue that can arise when comparing polarization curves obtained in different laboratories is represented by the flow rate applied to the fuel cell stack. It is well known, in fact, that mass transport limitations are dominant at high fuel utilization, thus the inlet flow rate provided to the stack represents a relevant parameter determining the resulting stack performance. In the present test module, the test is performed at constant fuel and air stoichiometry, i.e. the inlet flow rate is varied with the current variation. However, since for low current densities the resulting flow rate would be too low, a minimum flow rate is ensured to the stack during the test, i.e. the following condition is applied for both the anode and cathode:

$$\begin{cases} Q_{v,\lambda} = \dfrac{M}{zF\rho\varphi} n_{cell} I\lambda & \text{for} \quad \dfrac{M}{zF\rho\varphi} n_{cell} I\lambda > Q_{v,min} \\ Q_{v,\lambda} = Q_{v,min} & \text{for} \quad \dfrac{M}{zF\rho\varphi} n_{cell} I\lambda \le Q_{v,min} \end{cases} \tag{1}$$

where $Q_{v,\lambda}$ is the volumetric flow rate (dry basis) of the reactant considered, using a stoichiometric ratio λ, M is the molar mass of dry reactant gas, z is the number of exchanged electrons involved in the electrochemical reaction (2 for the anode, and 4 for the cathode), F is the Faraday constant, n_{cell} is the number of cells in the stack, ρ is the density of dry reactant gas under standard conditions, φ is the hydrogen or oxygen content in the dry gas mixture, and I is the current.

During the tests, the inlet flow rates and the current density are the variable inputs, while a number of other static inputs are defined in the test module. These include the composition of the inlet anodic and cathodic gas, stack temperature, stoichiometry, gas

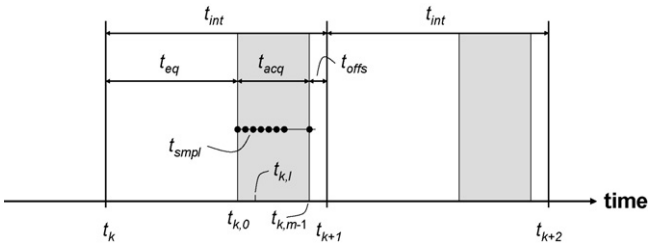

Fig. 2. Timeline for the data acquisition. Symbols are explained in Table 1.

inlet temperature, pressure and dew point temperature. The measured test outputs include: stack voltage, individual cell voltage, outlet gas temperature, coolant inlet–outlet temperature difference.

The test module also describes a general layout of the testing facility, and specifies the requirements in terms of maximum allowable uncertainty of the measuring system. However, no precise constriction of the test bench layout is provided. This is because the intention of the testing procedure is to be independent of the test bench used for the test. For more information on this specific test module, the reader is referred to the test module itself, publicly available at http://www.fctesqa.jrc.nl/.

The stack is first pre-conditioned, according to a procedure recommended by the stack manufacturer, or suggested in the test module. After a pre-conditioning phase of the stack, the polarization curve is recorded. This is obtained by stepwise increasing of the current density, and the relative flow rates after a pre-defined interval of time. Fig. 2 and Table 1 illustrate the data acquisition timeline. The value of the stack voltage reported at each point of the polarization curve is the mean value of those recorded during the acquisition time. It should be mentioned that the choice of having a pre-defined stabilization time is somewhat different from other existing testing procedures. The USFCC single cell protocol [30], for example, prescribes to "choose a stabilization time at each test point that includes the equilibration time for the test stand plus the fuel cell under test". The difference between the approach of FCTESTNET and USFCC is that the first refers to a convention, i.e. after a specific period of time, the acquisition is started, assuming that the equilibrium is in place; while in the latter, the acquisition cannot be started before the stabilization is achieved. The drawback of the first approach is that the values reported in the polarization curve might not represent accurate equilibrium points of the fuel cell (however, if the performance of different stacks are compared using the same procedure, it is not so relevant that the values should represent an equilibrium fuel cell state). With the second approach, the definition of the equilibrium arises, i.e. this should be quantitatively defined, in order to avoid that different organizations use different stabilization criteria. In Section 4.2, a more detailed understanding of the influence of the equilibrium time on the overall polarization curve is provided for an 11-kW stack.

Table 1
Time constants and variables related to data acquisition

Symbol	Description	Value	Unit
t_k	Start time of interval k, belonging to set point k		(s)
t_{int}	Interval between set points	15	(min)
t_{eq}	Equilibration time before start of data acquisition	10	(min)
t_{offs}	Interval between the end of the data acquisition time period for interval k ($t_{k,m-1}$) and beginning of next interval $k+1$	0.5	(min)
t_{acq}	Time period for data acquisition	$t_{int} - rkt_{eq} - t_{offs}$	(min)
t_{smpl}	Data acquisition sampling interval	10	(s)
m	Number of data points per interval k	$t_{acq}/t_{smp} + 1$	
$t_{k,l}$ ($0 \le l \le m-1$)	Data acquisition time points	$t_k + t_{eq} + lt_{smpl}$	(s)

For each set point k, m measurements of the test variables are taken and stored by the data acquisition software

Table 2
Test inputs

Input	Description	Range/value	Measurement uncertainty
I	Stack current density	0–1.6 A cm^{-2}	±2% for I < 0.1 A cm^{-2} ±1% for I > 0.1 A cm^{-2}
$Q_{v,fuel}$	Fuel flow rate	Corresponding to the stoichiometries (see Eq. (1))	±1% full scale
$Q_{v,ox}$	Oxidant flow rate	Corresponding to the stoichiometries (see Eq. (1))	±1% full scale
φ_{O_2}	Air oxygen concentration (dry basis)	0.21 m^3 O_2 per m^{-3} dry air	–
φ_{fuel}	Composition of fuel gas	100% H_2	+0/−0.005%
T_c	Inlet coolant temperature	60 °C	±1 °C
λ_{H_2}	Hydrogen stoichiometry	3 (non-dimensional)	–
λ_{Ox}	Air stoichiometry	4 (non-dimensional)	–
$T_{fuel,in}$	Fuel inlet temperature	50 °C	±1 °C
$T_{ox,in}$	Oxidant inlet temperature	50 °C	±1 °C
$T_{dew,fuel}$	Dew point of fuel gas	44 °C	±1 °C
$T_{dew,ox}$	Dew point of oxidant gas	44 °C	±1 °C

4. Results and discussion

4.1. Test module validation

The test module is applied to the PEFC stack described in Section 3. Since temperature distribution is far from uniform throughout the stack, the stack temperature is conventionally assumed to be equal to the coolant inlet.

Table 2 shows the value of the stack inputs during the test, while Fig. 3 shows the resulting polarization curve. The test was performed two times, with a time span of about 4 h between the two tests. In the second run, the resulting polarization curve (indicated with "Mean Stack Voltage 2", and Mean Stack power Density 2", in Fig. 3) is almost coincident with the previous one (the maximum difference is about 1.2%), thus demonstrating a good repeatability of the results.

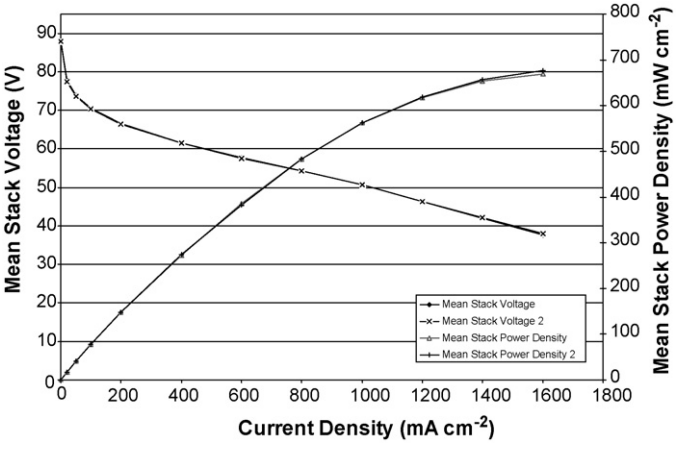

Fig. 3. Polarization curve of the 11 kW stack.

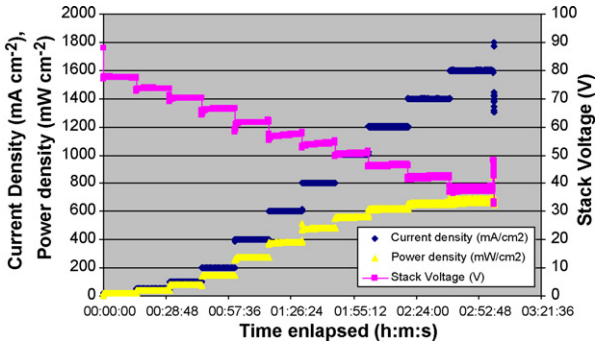

Fig. 4. Variation vs. time of the stack voltage, current density, and power density.

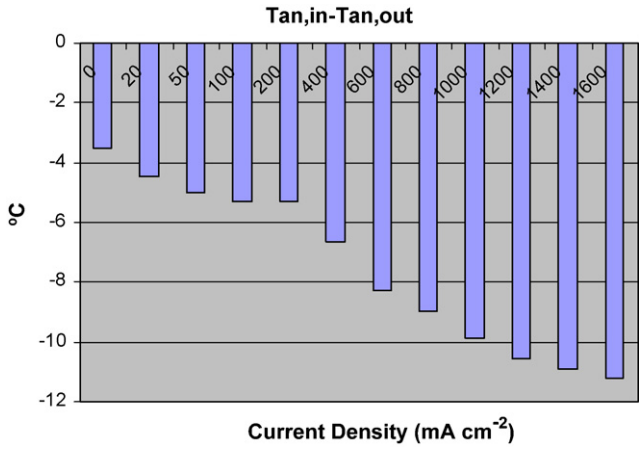

Fig. 5. Temperature difference between the inlet and the outlet of the anodic stream. The temperatures of the inlet and outlet streams are averaged vs. the acquisition time.

Fig. 4 shows the test results with respect to the time elapsed. The duration of the entire test is about 3 h. The test is stopped when at least one of the single cell voltages drops below 0.2 V.

4.2. Analysis of the results

It is very important to avoid any water condensation during the stack operation. This, in fact, would lead to electrode flooding and, consequently, to a rapid performance drop (e.g. [38–41]). Due to the high relative humidity of the inlet anodic and cathodic gas, if a temperature drop occurs, water condensation is likely to take place. Since heat is produced within the fuel cell as a consequence of the electrochemical reaction, a cooling water loop is present in the stack for maintaining a proper operating temperature. The temperature and flow rate of the cooling water need to be chosen so that heat removal is assured but without any reduction of the gas

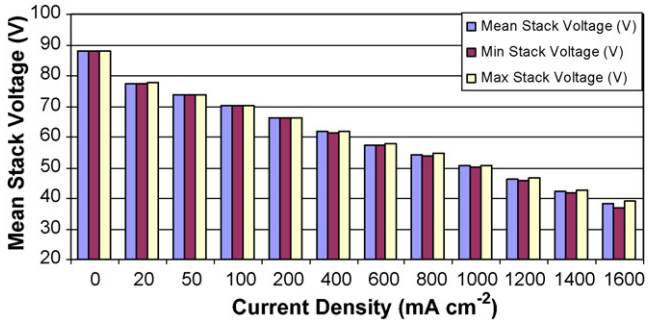

Fig. 6. Minimum, maximum. and mean stack voltage for different current densities.

temperature. With this aim, the temperatures of the inlet and outlet gases are continuously monitored. Fig. 5 shows the temperature difference between the inlet and the outlet of the anodic gas. The temperature difference of the cathodic gas presents a very similar trend, thus it is not reported. The increase of the temperature difference with increasing current density is due to the greater heat production by the fuel cell at higher current density. Fig. 5 also shows that the removal of heat from the stack is achieved by a com-

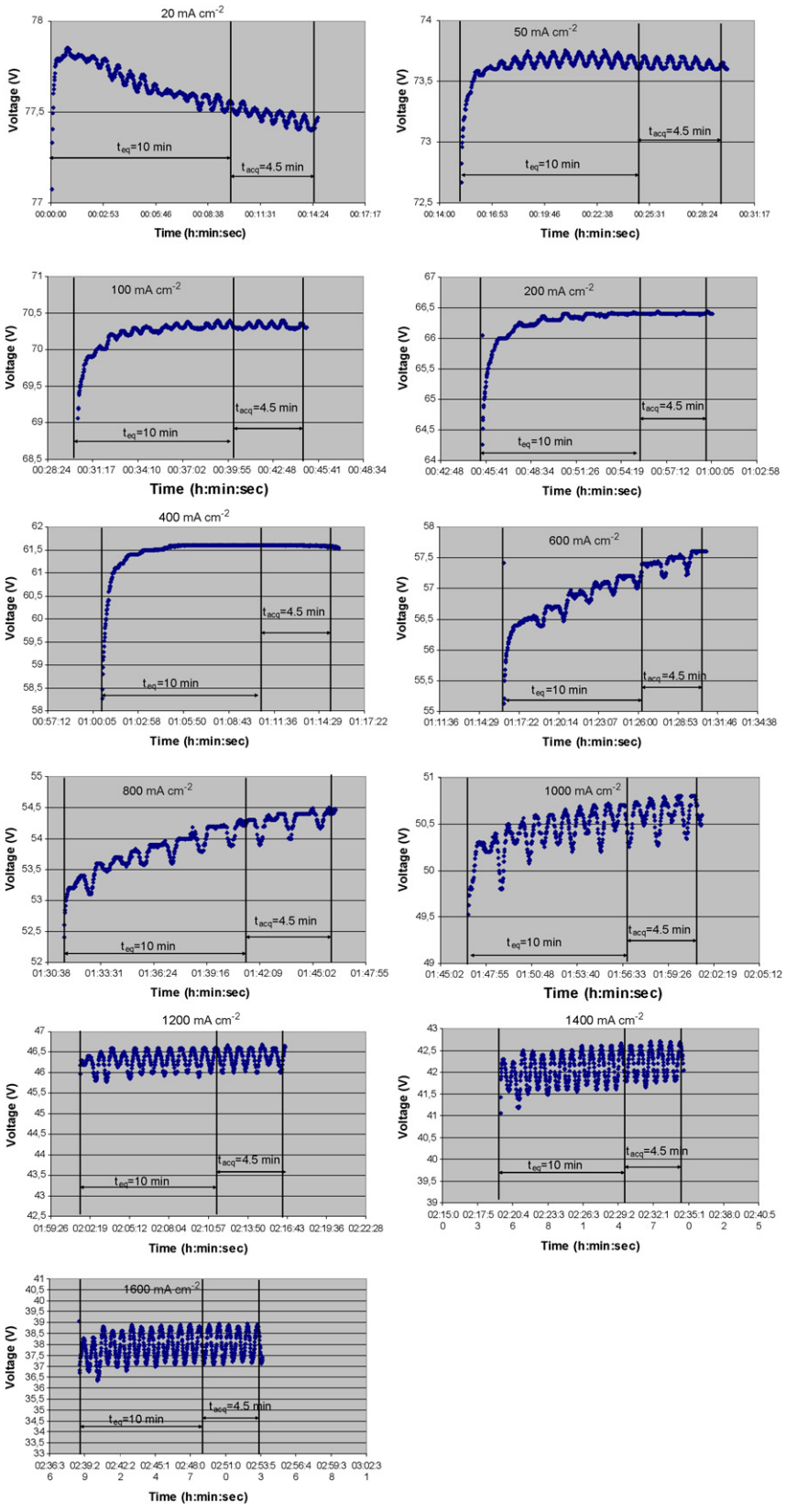

Fig. 7. Stack voltage vs. time for different current densities.

bination of the water-cooling loop and the temperature change of the anodic and cathodic gas. The temperature difference is negative for each current density imposed on the stack. This simple monitoring practice does not completely prevent water condensation, but it is a necessary measure. In a previous test performed on the same stack, under the same operating condition, but with a value of the inlet coolant temperature lower than the anodic inlet temperature, the stack showed much lower performance, and the voltage dropped very rapidly to zero. In such condition, it is very likely that water condensation takes place within the stack, thus leading to electrode flooding.

As previously mentioned, particular attention is given to the acquisition time and the results related to different acquisition times. Fig. 6 shows, for each current density, the maximum, minimum, and average stack voltage measured during the acquisition time. As expected, a voltage change with time occurs, especially for high current densities. In order to better understand the stack behavior reported in Fig. 6, the stack voltage versus time is plotted for each value of the current density (Fig. 7). The figure shows the stack voltage variation during the entire elapsed time, i.e. equilibrium plus acquisition time. It should be noticed that the test module foresees to acquire data only during the acquisition time, however, in order to have a better understanding of the stack behavior, the acquisition was performed during the entire duration of the test. Each graph of Fig. 7 represents the stack voltage soon after the current is increased. In each case, the voltage starts from a lower value, which represents the first response of the stack to the current increase, and, within few seconds, this increases to a higher value [42,43]. After this first response, the voltage variation results as the superposition of a periodic fluctuation, on a "long-term" steady

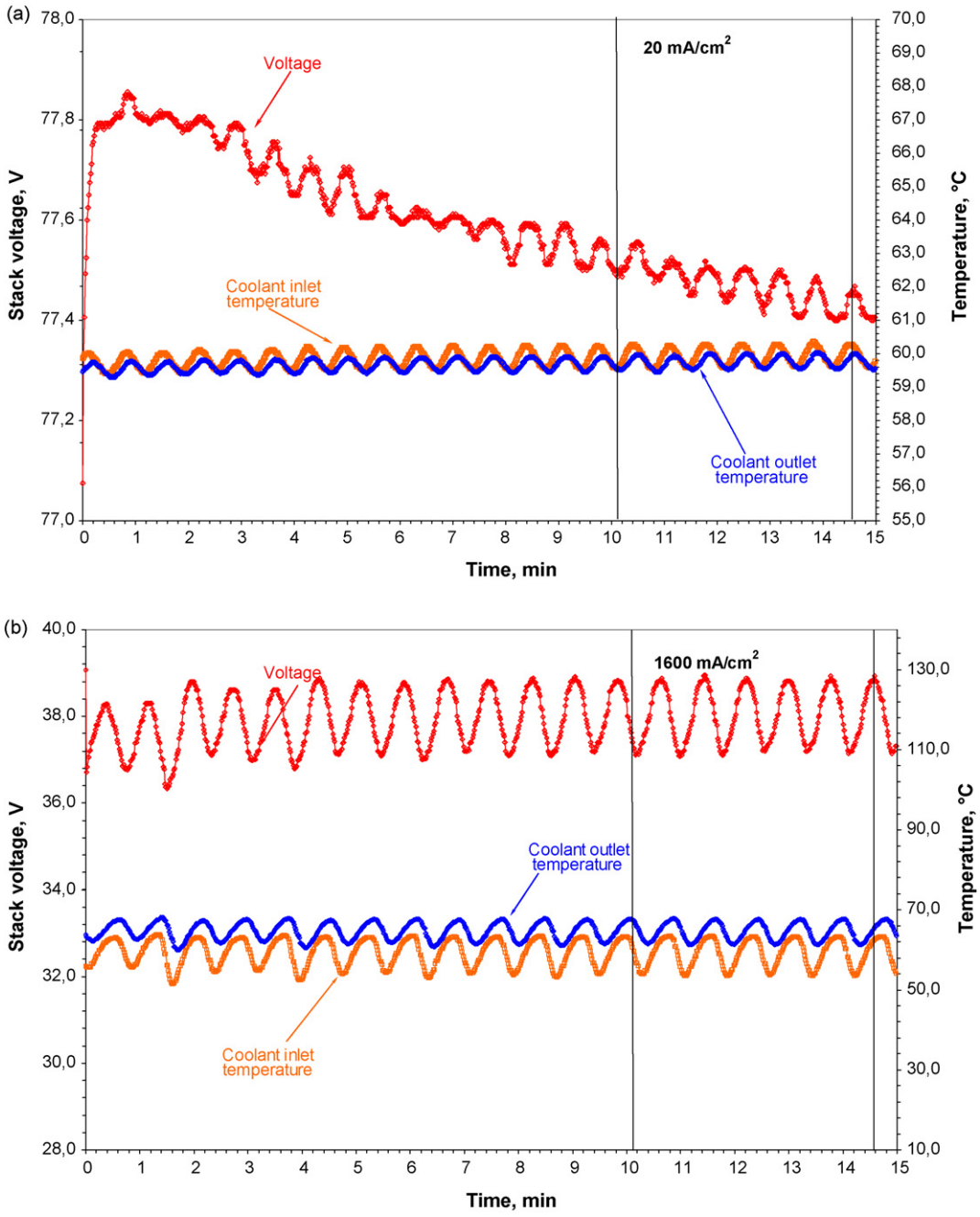

Fig. 8. Correlation between stack voltage and coolant temperature, when the current density is (a) 20 mA cm^{-2} and (b) 1600 mA cm^{-2}.

variation. In all cases, the voltage variation during the acquisition time is below 4%. When the current density increases, the long-term voltage change decreases, while the fluctuation increases in its amplitude.

Slow voltage variations are due to chemical reactions occurring within the stack, and to the related long time associated to the equilibrium of the gas and liquid phases within the stack, particularly in the hydration/dehydration process of the cell membranes [44]. Therefore, such voltage variation is mostly technology-dependent, and is not due to the test method. On the other hand, the periodic stack voltage fluctuation suggests an external cause, which must be considered in the testing procedure. In order to identify a correlation between such fluctuation and the test inputs, all the inputs specified in Table 2 have been acquired during the test, and plotted versus time, together with the stack voltage. Such exercise allowed for the correlation of the stack voltage fluctuation with the coolant temperature, as shown in Fig. 8. This correlation suggests that the discrepancy between the nominal and the real value of the coolant temperature must be carefully controlled and maintained within a certain range, during the tests. In the case of Fig. 8(a), a fluctuation of the inlet coolant temperature of about 2% (on °C) results in a voltage fluctuation of less than 0.5%, while in the case of Fig. 8(b), a temperature fluctuation of about 18% produces a voltage fluctuation of about 4.8%.

By assuming that the temperature variation within the present range affects mainly the ohmic resistance of the stack, it is possible to correlate the change of the stack voltage with the change of the ohmic resistance, due to the temperature variation. Ohmic losses can be expressed as

$$\eta_{ohm} = Z_{ohm} \cdot J_{cell} \tag{2}$$

where Z_{ohm} is the resistance of the stack, namely:

$$Z_{ohm} = Z_{mem} + Z_{cont} + Z_{GDL} + Z_{CC} \tag{3}$$

In expression (3), Z_{mem} represents the protonic resistance of the membrane, Z_{con} the contact resistance between different single cells and between the different layers of a single cell, Z_{GDL} is the resistance of the gas diffusion layer, and Z_{CC} the resistance of the current collector. As the resistance of the current collectors and the gas diffusion layer are negligible compared to Z_{mem} and Z_{cont} [45], and considering the contact resistance independent of the temperature, expression (3) becomes:

$$Z(T_1) - Z(T_2) = \Delta Z = Z_{mem}(T_1) - Z_{mem}(T_2) = \Delta Z_{mem} \tag{4}$$

The conductivity of the membrane can be computed as [46]

$$\kappa = (0.005139\xi - 0.00326)\exp\left[1268\left(\frac{1}{303} - \frac{1}{T}\right)\right] \tag{5}$$

with

$$\xi = 0.043 + 17.81a - 39.85a^2 + 36a^3 \tag{6}$$

where a represents the water activity.

When the stack current is varied, the fluctuation of the coolant temperature at the outlet changes, as a consequence of the change of the heat released by the electrochemical reaction. A lumped value of the stack temperature is assumed here, i.e. the average between the coolant inlet and outlet temperature. Table 3 reports, for different current densities, the maximum stack temperature difference, and the related resistance change, measured during the acquisition time t_{eq}.

Under the assumptions that lead to Eq. (4), and considering the well-known Ohm's law, the variation of the resistance, related to the operating conditions of Table 3 can be computed:

$$Z(T_1) - Z(T_2) = \Delta Z = \frac{V(T_1) - V(T_2)}{J_{cell}} \tag{7}$$

Table 3
Maximum stack temperature difference, and the related resistance change, measured during the acquisition time t_{eq}

Current density, J (A cm^{-2})	ΔT (K)	$\Delta R_{exp} = \Delta V/J$ (Ω cm)
0.2	0.71	0.17
0.8	3.2	0.5
1.4	5.27	0.61
1.6	8.25	0.76

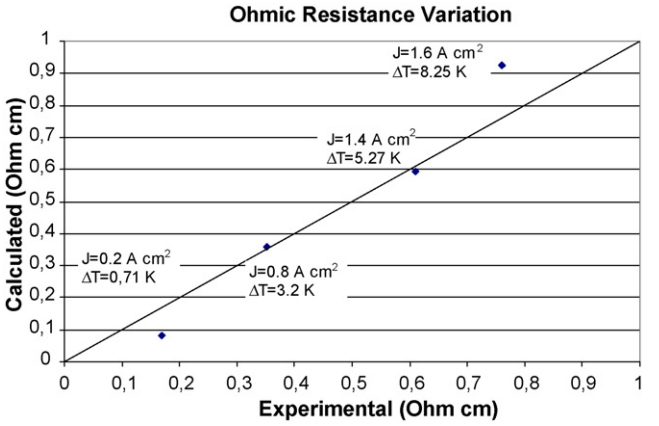

Fig. 9. Comparison between calculated and experimental variation of the stack resistance at different stack conditions (ΔT represents the maximum variation of the stack temperature, lumped as the average between the inlet and outlet coolant temperature).

The obtained values of ΔZ(experimental) are compared to those calculated via Eqs. (4)–(6), assuming a fully hydrated membrane ($a = 1$, thus $\xi = 14$). As shown in Fig. 9, there is a reasonable agreement between calculated and experimental results.

In order to further validate the assumptions of considering the variation of the ohmic resistance, as the main cause of the voltage fluctuation, all the three main voltage losses are considered (namely, activation, ohmic and concentration losses), and their magnitudes are compared to each other.

Assuming that every cell in the stack exhibits the same performance, the stack voltage can be calculated as [47]

$$V = n_{cells} V_{cell} \tag{8}$$

where

$$V_{cell} = \frac{OCV_{stack}}{n_{cell}} - b\ln(J_{cell}) - \eta_{conc} - \eta_{ohm} \tag{9}$$

$$\eta_{conc} = J_{cell} \cdot A\exp\left(\frac{1}{T_m - T}\right) \tag{10}$$

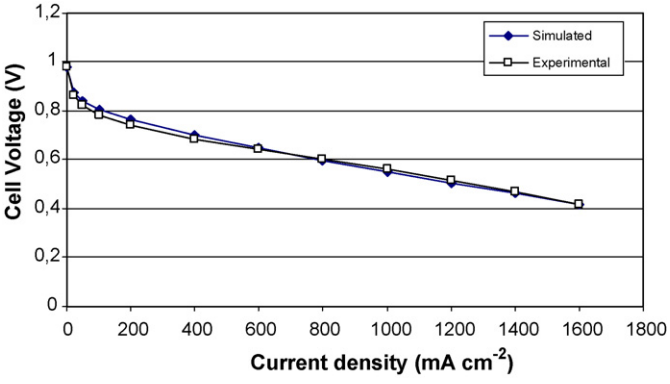

Fig. 10. Comparison between experimental and calculated cell voltage.

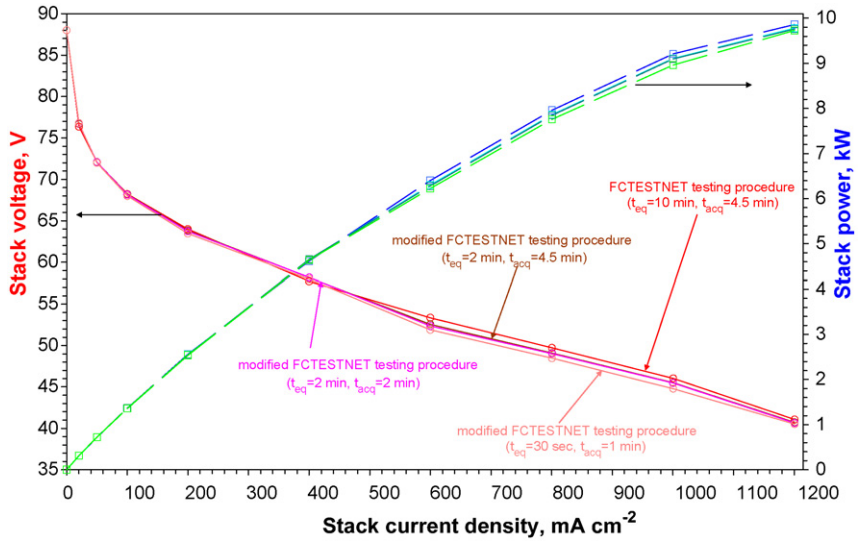

Fig. 11. Comparison of the polarization curves relative to different equilibrium and acquisition times.

Table 4
Parameters used in expressions (2)–(10) in computing the results depicted in Fig. 11

Parameter	Value	Unit of measurement
Water activity (a)	1	–
Tofel slope (b)	0.033	V
A	0.004077	$\Omega\,cm^2$
T_m	42	°C
OCV_{stack}	88.2	V
n_{cell}	90	–

In expressions (8)–(10), n_{cell} is the number of the cells in the stack, OCV_{stack} is the open circuit voltage of the stack, b is the Tafel slope, A is an empirical parameter, and T_m represents the stack temperature above which mass-transfer overvoltage initiates [47].

Fig. 10 depicts the comparison between the experimental data, and those computed through (8)–(10), using the data reported in Table 4.

The next step is to assess the effect of temperature variation on the voltage loss. This analysis is performed by considering 335 K as the baseline, and calculating the variation of the voltage loss when the temperature is increased by 1, 5 and 10 K.

Results for two current densities (namely $J_{cell} = 100$ and 1600 mA cm^{-2}) are reported in Table 5. Since, within the approach used in expression (9), the activation overpotential is not dependant on temperature, only the variation of ohmic and concentration losses are reported. The results confirm that, under the present operating conditions, a variation of the stack temperature within 10 K produces a variation of the stack voltage mostly due to the change of the membrane conductivity.

Table 5
Variation of ohmic and concentration loss when temperature is increased by 1, 5, and 10 K, from 335 K

	ΔT (K)		
	1	5	10
$J_{cell} = 100$ mA cm^{-2}			
$\Delta\eta_{ohm}$ (V)	2.186E−4	1.057E−3	2.028E−3
$\Delta\eta_{conc}$ (V)	1.26E−9	6.29E−9	1.25E−8
$J_{cell} = 1600$ mA cm^{-2}			
$\Delta\eta_{ohm}$ (V)	3.5E−3	16.91E−3	0.03245
$\Delta\eta_{conc}$ (V)	2.03E−8	1.01E−7	2E−7

As Fig. 2 and Table 1 show, each value of the current density requires a total time of 15 min before increasing the current to the next value. For the present case, where the maximum current density is 1600 mA cm^{-2}, the time required to complete the polarization curve is about 3 h. To this time, start-up and preconditioning time should also be added. Moreover, if a reverse polarization curve is also performed (i.e. obtained by decreasing the current density from the maximum value to OCV), more than 6 h are required to complete the test. Since polarization curves are usually conducted as routine tests (e.g. to quantify performance degradation after a defined amount of time), or as a quick acceptance test in an industrial environment, such a long execution time might represent a major issue. For this reason, the same test was repeated, using shorter equilibrium and acquisition times. Fig. 11 shows the resulting polarization curves for the following cases:

1. Base case (indicated as FCTESTNET procedure);
2. Equilibrium time of 2 min and acquisition time of 4.5 min;
3. Equilibrium time of 2 min and acquisition time of 2 min;
4. Equilibrium time of 30 s and acquisition time of 1 min.

Results show that the largest deviation from the base case, arising at 600 mA cm^{-2} for case 4, is still acceptable, i.e. 0.4%. Therefore, the equilibrium and acquisition time can be drastically reduced from 15 min to about 1.5 min. In the present case, the total execution time is reduced from 3 h to about 20 min. Such reduction of the execution time, if considered in a mass production context, represents a strong cost reduction, and resources saving in an R&D laboratory.

5. Conclusions and final remarks

In the present paper, a preliminary experimental validation of a test module developed within the framework of the EU-funded project FCTESTNET is presented. The test module, concerning the polarization curve of a PEM stack was applied to a stack composed of 90 single cells, with a nominal power of 11 kW_e.

The experimental campaign revealed some important factors to consider in the test module itself. First, the temperature of the coolant is observed to affect the stack voltage, thus the test module needs to specify a maximum allowable deviation from the nominal value. In the present case, a temperature variation of about 2% of the coolant produces a voltage fluctuation of less than 0.5%. Second,

the equilibrium and acquisition time showed a very limited impact on the final polarization curve when reduced from 10 min to 30 s for the equilibrium time, and from 4.5 min to 1 min for the acquisition time. This observation will allow a substantial reduction of the overall testing time, thus allowing for a reduced employment of resources for executing the tests.

Finally, it is important to observe that, before arriving to a final definition of the testing procedure, the present tests should be repeated on a different stack and, possibly, using a different test hardware, in order to exclude any dependency of the results on the specific technology employed.

Acknowledgements

This work has been carried out under the Framework Program 6 (FP6) Multi Annual Work Program (MAWP) 2003–2006 of the Joint Research Centre within the Fuel Cells Performance Testing Action (F02-30; 2322) of the Institute for Energy.

The authors would like to thank Dr. Mauro Scagliotti of Cesi Ricerche for the review of the International standardization activities and all the partners of FCTESTNET and FCTES^{QA}.

References

[1] G. Tsotridis, A. Podias, W. Winkler, M. Scagliotti, FCTESTNET Fuel Cells Glossary, EUR Report 22295 EN, Scientific and Technical Research Series, Office for Official Publications of the European Communities, Luxembourg, ISBN 92-79-02747-6, 2006.
[2] K.S. Dhathathreyan, N. Rajalakshmi, in: S. Basu (Ed.), Recent Trends in Fuel Cell Science and Technology, Springer, 2007, pp. 40–115.
[3] J.S. Wainright, R.F. Savinelli, C.C. Liu, M. Litt, Electrochim. Acta 48 (20–22) (2003) 2869–2877.
[4] J. Zhang, Z. Xie, J. Zhang, Y. Tang, C. Songa, T. Navessin, Z. Shi, D. Songa, H. Wang, D.P. Wilkinson, Z.-S. Liu, S. Holdcroft, J. Power Sources 160 (2006) 872–891.
[5] F.-B. Weng, B.-S. Jou, A. Su, S.H. Chan, J. Power Sources 171 (2007) 179–185.
[6] P. Yu, M. Pemberton, P. Plasse, J. Power Sources 144 (1) (2005) 11–20.
[7] J.L. Cohen, D.A. Westly, A. Pechenik, H.D. Abruña, J. Power Sources 139 (1–2, 4) (2005) 96–105.
[8] M.G. Santarelli, M.F. Torchio, Energy Conv. Manage. 48 (1) (2007) 40–51.
[9] M.V. Williams, H.R. Kunz, J.M. Fenton, J. Power Sources 135 (1-2) (2004) 122–134.
[10] A. de Souza, E.R. Gonzalez, J. Solid State Electrochem. 7 (9) (2003) 517–664.
[11] F. Rinaldi, R. Marchesi, J. Fuel Cell Sci. Technol. 4 (3) (2007) 231–237.
[12] International Electrochemical Commission, Technical Specification IEC/TS 62282-1 (2005-03), Fuel Cell Technologies (TC 105)—Part 1. Terminology, 2005.
[13] International Electrochemical Commission, International Standard IEC 62282-2, Fuel Cell Technologies (TC 105)—Part 2. Fuel Cell Modules, 2004.
[14] International Electrochemical Commission, Publicly Available Specification IEC PAS 62282-6-1, Fuel Cell Technology (TC 105)—Part 6-1. Microfuel Cell Power Systems Safety, 2006.
[15] International Electrochemical Commission, International Standard IEC 62282-3-2 (2006-03), Fuel Cell Technologies (TC 105)—Part 3-2. Stationary Fuel Cell Power Systems: Performance Test Methods, The Document has Been Adopted as a European Standard as EN 62282-3-2:2006, 2006.
[16] American National Standard Institute, American National Standard ANSI/CSA FC1-2004 Stationary Fuel Cell Power Systems (formerly ANSI Z21.83 Fuel Cell Power Plants), 2004.
[17] The American Society of Mechanical Engineers, American National Standard ASME PTC 50-2002, Fuel Cell Power Systems Performance, 2002.
[18] National Fire Protection Association, NFPA 853 Standard for the Installation of Stationary Fuel Cell Power Plants, 2003.
[19] Japanese Industrial Standard, Japanese National Standard JIS C 8800:2000 Glossary of Terms for Fuel Cell Power Systems, 2000.
[20] Japanese Industrial Standard, Japanese National Standard JIS C 8801:2002 General Rules for PAFC Power Generating System packaged of 50 to 500 kW, 2002.
[21] Japanese Industrial Standard, Japanese National Standard JIS C 8802:2003 Accelerated Test Methods for Phosphoric Acid Fuel Cell, 2003.
[22] Japanese Industrial Standard, Japanese National Standard JIS C 8803 Indication of PAFC Power Facility, 2005.
[23] Japanese Industrial Standard, Japanese National Standard JIS C 8811:2005 Indication of Polymer Electrolyte Fuel Cell Power Facility, 2005.
[24] German Technical and Scientific Association for Gas and Water (DVGW), Industrial Rule VP119 Preliminary Basic Rules for Construction, Functional Requirements and Installation of Fuel Cell Gas Appliances with a Maximum Heat Input (gas flow) of 70 kW, 2000.
[25] Society of Automotive Engineers, Recommended Practice J2615 Performance Test Procedure of Fuel Cell Systems for Automotive Applications, 2005.
[26] Society of Automotive Engineers, Recommended Practice J2594 Recommended Practice to Design for Recycling Proton Exchange Membrane (PEM) Fuel Cell Systems, 2003.
[27] Society of Automotive Engineers, Recommended Practice J2578 Recommended Practice for General Fuel Cell Vehicle Safety, 2002.
[28] Society of Automotive Engineers, Information Report J2574 Fuel Cell Vehicle Terminology, 2002.
[29] US Fuel Cell Council, USFCC Protocol on Fuel Cell Component Testing: Primer for Generating Test Plans (USFCC 04-003), 2004.
[30] US Fuel Cell Council, Single cell Protocol, document number UFCC 05-014, 2005.
[31] M.W. Davis, M.W. Ellis, B.P. Dougherty, Proposed Test Methodology and Performance Rating Standard for Residential Fuel Cell Systems. NISTIR 7131, 2006.
[32] R. Friberg, R. Winkel, R. Smokers, D. Foster, L. Joerissen, G. Tsotridis, W. Winkler, A. Podias, C. Voight, A Proposal of a Harmonised Testing Format for Fuel Cell Technology—FCTESTNET (Paper 74068), in: American Society of Mechanical Engineers (ASME) Proceedings of FUELCELL2005 Third International Fuel Cell Conference on Fuel Cell Science, Engineering and Technology, Ypsilanti, MI, USA, May 23–25, 2005.
[33] Y. Hashimasa, T. Numata, K. Moriya, S. Watanabe, J. Power Sources 155 (2) (2006) 182–189.
[34] Japanese Automotive Research Institute (JARI) and the Japan Electrical Manufacturers' Association (JEMA), Single Cell Test Method for Polymer Electrolyte Fuel Cell (PEFC). Draft Version 1.0, 2006.
[35] S. Watanabe, Second FCTESTNET workshop, Ulm, Germany, October 22nd, 2004.
[36] S. Watanabe, M. Tatsumi, M. Akai, Proceedings of the 2004 Fuel Cell Seminar, San Antonio, TX, November 2–5, 2004.
[37] Y. Hashimasa, N. Yoshimura, D. Ebata, H. Tomioka, M. Akai, S. Watanabe, K. Bethune, R. Rocheleau, Proceedings of the Fifth International Conference on Fuel Cell Science Engineering and Technology, Brooklyn, NY, June 18–20, 2007.
[38] K. Ito, in: S. Basu (Ed.), Recent trends in Fuel Cell Science and Technology, Springer, 2007, pp. 129–136.
[39] F. Barbir, PEM Fuel Cells: Theory and Practice, Elsevier-Academic Press, 2005.
[40] F. Barbir, H. Gorgun, X. Wang, J. Power Sources 141 (2005) 96–101.
[41] A. Hakenjos, H. Muenter, U. Wittstadt, C. Hebling, J. Power Sources 131 (2004) 213–216.
[42] J.C. Amphlett, B.A. Mann, P.R. Roberge, A. Rodrigues, J. Power Sources 61 (1996) 183–188.
[43] X. Yan, M. Hou, L. Sun, H. Cheng, Y. Hong, D. Liang, Q. Shen, P. Ming, B. Yi, J. Power Sources 163 (2007) 966–970.
[44] F. Yang, R. Pitchumani, in: N.M. Sammes (Ed.), Fuel Cell Technology, Reaching Towards Commercialization, Springer-Verlag, London, 2006, pp. 69–163.
[45] D. Gerteisen, et al., J. Power Sources 177 (2008) 348–354.
[46] T.E. Springer, T.A. Zawodzinski, S. Gottesfeld, J. Electrochem. Soc. 138 (8) (1991) 2334–2342.
[47] R. Jiang, D. Chu, J. Power Sources 92 (2001) 193–198.